JOURNAL OF CATALYSIS 75, 251–261 (1982)

Effects of Dispersion on the Activity and Selectivity of Alumina-Supported Ruthenium Catalysts for Carbon Monoxide Hydrogenation

C. STEPHEN KELLNER AND ALEXIS T. BELL

Materials and Molecular Research Division Lawrence Berkeley Laboratory and Department of Chemical Engineering University of California, Berkeley, California 94720

Received March 27, 1981; revised December 29, 1981

A study was performed to determine the extent to which metal dispersion affects the activity and selectivity of Ru/Al_2O_3 catalysts used for CO hydrogenation. For dispersions below 0.7, the specific activity for synthesis of methane and C_{2+} products decreases with increasing dispersion, but neither the probability for chain growth nor the olefin-to-paraffin ratio is affected. The decrease in activity over this range is ascribed to a decrease in the fraction of sites present on planar surfaces. For dispersions above 0.7, the specific activity for synthesis of all products decreases dramatically, and is accompanied by a slight decrease in the probability of chain growth and a rapid decrease in the olefin-to-paraffin ratio. These changes are attributed to changes in the electronic properties of the Ru microcrystallites with size and the occurrence of metal/support interactions. *In situ* infrared spectra reveal that only those sites that adsorb one linearly bound CO molecule per Ru atom are active for CO hydrogenation. Adsorption of two CO molecules per Ru site is also observed but these site are catalytically inactive.

INTRODUCTION

The influence of dispersion on the performance of supported Group VIII metals for the synthesis of hydrocarbons via CO hydrogenation has been studied to only a limited degree. Vannice (*1, 2*) has reported that the specific activity for methanation of Pt and Pd catalysts increases with increasing dispersion, the effect being much more dramatic for Pt than Pd. By contrast, the methanation activity of Ni catalysts was found to decrease with increasing dispersion. Dalla Betta *et al.* (*3*) observed a similar trend for Ru/Al_2O_3 catalysts. In a more detailed study, King (*4*) reported that the specific activities of supported Ru catalysts for methanation and CO consumption decreased monitonically with increasing Ru dispersion. No correlation was noted, though, between the distribution of hydrocarbon products and dispersion.

In the present study, an investigation of the effects of dispersion on the characteristics of Ru/Al_2O_3 catalysts for hydrocarbon synthesis was undertaken. Emphasis was placed on defining the effects of Ru dispersion on specific activity, product distribution, and olefin-to-paraffin ratio of the products. In addition to analysis of reaction products, *in situ* infrared spectroscopy was used to characterize the structure of chemisorbed CO as a function of catalyst dispersion.

EXPERIMENTAL

Three γ-alumina-supported catalysts were used in this investigation. A 1.3% Ru/Al_2O_3 catalyst was prepared by adsorption of $Ru_3(CO)_{12}$ from pentane solution (*5*). The dried catalyst was reduced in flowing H_2 at 1 atm. Reduction was begun by raising the temperature from 298 to 673 K after which the temperature was maintained at 673 K for 8 hr. The dispersion of the reduced catalyst was measured by H_2 chemisorption and determined to be 0.9. Two catalysts, a 3.0% Ru/Al_2O_3 and an 11% Ru/Al_2O_3 catalyst were prepared by incipient wetness impregnation of the support with an aqueous solution of $RuCl_3$, acidified to pH = 2 to sup-

0021-9517/82/060251-11$02.00/0

press hydrolysis. The resulting slurry was air dried and then heated slowly in vacuum from 298 to 423 K. Reduction of these catalysts was carried out using the procedure described for the 1.3% Ru/Al_2O_3 catalyst. The dispersion of the 3.0% Ru/Al_2O_3 catalyst, determined by H_2 chemisorption, was 0.5 and that of the 11% Ru/Al_2O_3 catalyst was 0.3.

Investigations of catalyst activity were conducted at 1 and 10 atm. The low-pressure studies were carried out in a glass microreactor connected to a glass vacuum and gas handling system. The design of this apparatus allowed measurements of synthesis activity and H_2 isotherms to be performed in the same cell. The flow of synthesis gas—a preblended H_2/CO mixture ($H_2/CO = 2$)—to the reactor was controlled by a needle valve and measured using a bubble flow meter. Analysis of the reaction products was carried out by gas chromatography using flame ionization detection of the eluted components. Products in the C_1 through C_5 range were separated using a 1 m × 2.4 mm stainless-steel column packed with Chromsorb 106. A 2.5-cm^3 sample was injected into the column maintained at 318 K. The column temperature was then programmed to 478 K at 10 K/min. Separation of C_4 through C_{14} products was carried out using a 50 m × 0.25 mm fused silica column coated with SE-54. A modified Grob injection (*6*) was used to introduce the sample. With the column at 193 K, a 10-cm^3 gas sample was injected at a split ratio of 20 : 1. The column was held at 193 K for 5 min and then programmed at 5 K/min to 478 K.

High-pressure studies were conducted in a stainless-steel microreactor which also served as an infrared cell. The design of this cell is similar to that recently described by Hicks *et al.* (*7*). Synthesis gas was supplied to this reactor from a high-pressure manifold, and products were analyzed by gas chromatography. These portions of the apparatus have been described previously (*8, 9*).

Infrared spectra were taken with a Digilab FTS-10M Fourier transform infrared spectrometer at a resolution of 4 cm^{-1}. Typically, 100 interferograms, each acquired in 1.25 s, were coadded to improve the signal-to-noise ratio. In addition to recording spectra of the catalyst under reaction conditions, spectra were also recorded of the catalyst following reduction in H_2 and of a support disk, placed downstream of the catalyst disk, during reaction. The latter two spectra were used to substract out infrared absorptions due to the support and the gas phase.

RESULTS

Catalyst Activity and Selectivity

Experiments conducted with the 1.3% Ru/Al_2O_3 catalyst revealed that the dispersion of this catalyst decreased under reaction conditions from its initial value of 0.9. To determine how the progressive change in metal dispersion affected the activity and selectivity of the catalyst, a series of short duration runs were performed at 1 atm in the cell used to obtain H_2 isotherms. Approximately 800 mg of the catalyst (+120, −80 Mesh) were placed in the cell, evacuated to 2 × 10^6 Torr at 373 K, and then reduced in flowing H_2. During reduction, the catalyst was heated to 623 K at 1 K/min and then maintained at 623 K for 2 hr. Following reduction, the cell was again evacuated and the temperature was reduced to 373 K. An H_2 isotherm was then determined at 373 K. Next, the cell was once more evacuated and, after reducing the temperature to 297 K, a preblended H_2/CO mixture ($H_2/CO = 2$) was passed over the catalyst at 1 atm and 100 cm^3/min (NTP) for 10 min. At the end of this time, the cell temperature was increased to 477 K over a 5-min interval. After 20 min at temperature, gas samples were taken for analysis. The reaction was then terminated and the cell evacuated. The catalyst was then reduced, following the procedure described earlier, and a new H_2 isotherm was determined in preparation for a subsequent reaction run. The complete procedure was repeated six

times, at the end of which it was observed that the catalyst had attained a relatively stable dispersion of 0.6. Similar reaction and reduction cycles were also carried out with a 50-mg sample of the 11% Ru/Al_2O_3 catalyst. The activity of this catalyst was stable and, therefore, it was assumed that the catalyst dispersion did not decrease with use. It should be noted that in all instances the conversion of CO never exceeded 2% with either catalyst.

The effect of dispersion on the turnover number for methane synthesis, N_{C_1}, is shown in Fig. 1. With the exception of the point for $D_{Ru} = 0.3$, which was obtained using the 11% Ru/Al_2O_3 catalyst, all of the data were collected using the 1.3% Ru/Al_2O_3 catalyst. The points plotted in Fig. 1 are based on the average dispersion pertaining to a 20-min period of reaction. In those cases where a change in dispersion occurred during a reaction cycle, the initial and final dispersions are indicated by vertical bars. The results presented in Fig. 1 clearly show that as dispersion increases, the turnover number for methane synthesis rapidly declines. It is also apparent that the data lie along two line segments which meet near $D_{Ru} < 0.75$ and that the absolute magnitude of the slope of the segment for $D_{Ru} < 0.75$ is significantly lower than the magnitude of the slope of the segment for $D_{Ru} > 0.75$.

For the sake of comparison with the present results, King's data (*4*) for unsupported Ru and for alumina-supported Ru have also been shown in Fig. 1. It is evident that the data for both the supported and unsupported metal lie along a common line and that the slope of that line is nearly identical to that obtained in the present study for catalysts with Ru dispersions below 0.75. The vertical displacement of King's data is due to the higher pressure and temperature used in his study.

Figure 2 shows that with decreasing dispersion the specific activity for the synthesis of C_2 through C_{14} hydrocarbons increases in a manner similar to that observed for methane. In this figure, the turnover number, N_{C_n}, for producing a product con-

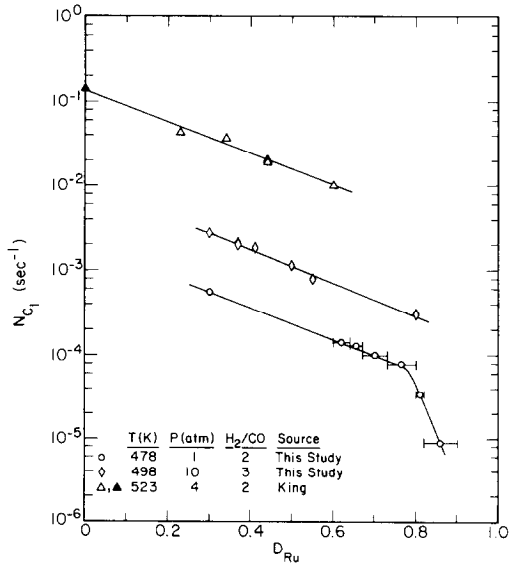

FIG. 1. Effect of dispersion on the specific activity for methane formation over alumina-supported (○, ◇, △) and unsupported (▲) Ru.

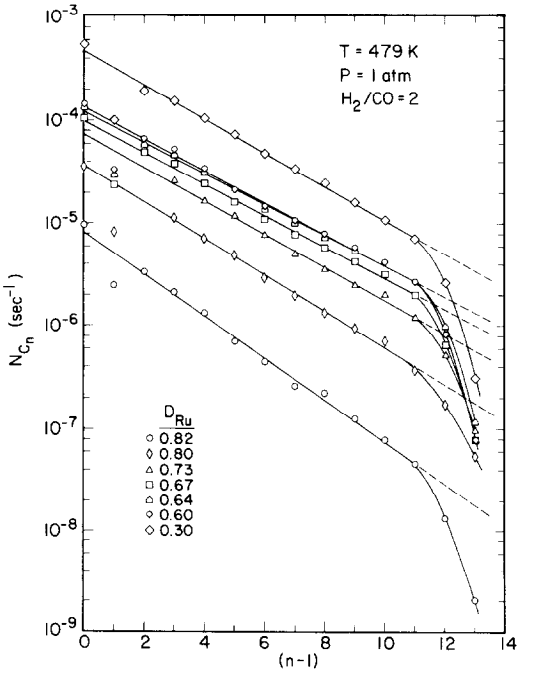

FIG. 2. Effects of dispersion on the rates of formation and the distribution of hydrocarbons over alumina-supported Ru.

taining n carbon atoms is based on the dispersion determined at the end of a 20-min period of reaction. Note that for each dispersion the majority of the points lie along a straight line on the coordinates of $\ln(N_{C_n})$ versus $(n - 1)$ as would be expected if chain growth occurs via a stepwise polymerization type mechanism (*9, 10*). The only points that fail to lie along the straight lines are those for $n = 2$ and for $n \geq 13$.

Figure 3 shows that the extent of deviation of the points for $n \geq 13$, from a log-normal product distribution, strongly depends on the reactant flow rate and the time at which a product sample is taken for analysis. As either the flow rate or the time of reaction is increased, the extent of deviation decreases significantly. Similar observations were also made for runs conducted at 10 atm, in which case deviations from a log-normal product distribution were seen for $n > 5$.

The slope of the straight lines shown in Fig. 2 is equal to log α, where α is the probability of hydrocarbon chain growth (*9, 10*). Table 1 shows that the magnitude of α increases slightly from 0.63 to 0.7 as the dispersion, measured after reaction, decreases from 0.82 to 0.67. Thereafter, α remains constant at a value of about 0.7.

TABLE 1

Effects of Dispersion on the Probability of Chain Growth[a]

i	$D_{Ru}^{(i-1)}$ [b]	$D_{Ru}^{(i)}$ [c]	α
1	0.90	0.82	0.63
2	0.82	0.80	0.66
3	0.80	0.73	0.69
4	0.73	0.67	0.70
5	0.67	0.64	0.71
6	0.64	0.60	0.70
7[d]	0.30	—	0.69

[a] Reaction conditions $T = 479$ K; $P = 1$ atm; $H_2/CO = 2$. catalyst: 1.3% Ru/Al_2O_3.
[b] Measured before reaction cycle i.
[c] Measured after reaction cycle i.
[d] Catalyst: 11% Ru/Al_2O_3.

Figure 4 illustrates the effect of dispersion on the olefin-to-paraffin ratio of prod-

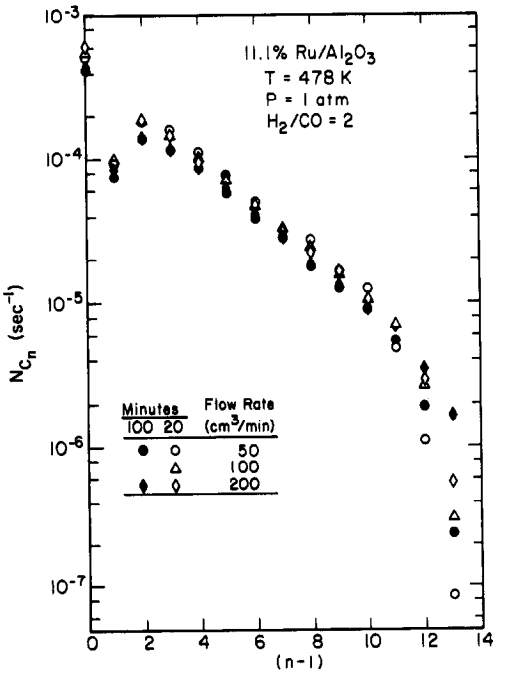

FIG. 3. Effects of flow rate and time of reaction on the rates of formation of hydrocarbon products over alumina-supported Ru.

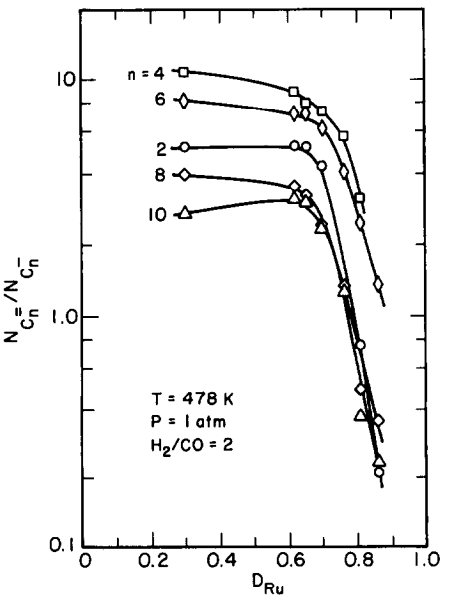

FIG. 4. Effect of dispersion on the olefin to paraffin ratio of hydrocarbon containing 2, 4, 6, 8, and 10 carbon atoms formed over alumina-supported Ru.

ucts containing 2, 4, 6, 8, and 10 carbon atoms. In each case the ratio, N_{C_n}/N_{C_n-}, is found to be weakly dependent on dispersion for dispersions below about 0.6 to 0.7. For higher dispersions, the ratio drops precipitously, indicating the formation of a very paraffinic product. While not shown, similar results were obtained for products containing 3, 5, 7, 9, 11, 12, 13, and 14 carbon atoms.

Infrared Spectroscopy

Infrared spectra of the carbonyl stretching region were taken both during reaction and during subsequent reduction of the catalyst. The majority of this effort was carried using the 1.3% Ru/Al_2O_3 catalyst and the following procedure. A freshly prepared catalyst disk was reduced *in situ* in flowing H_2 at 573 K and 10 atm for approximately 16 hr. The temperature was then decreased to 498 K and a mixture of H_2 and CO (H_2/CO = 3) was fed to the reactor. Reaction was allowed to proceed for 10 min. During the last 2 min of this period 100 interferograms were taken of the catalyst and coadded. At the end of the reaction period, the product gases were analyzed and the flow of synthesis gas was replaced by a flow of H_2. After 10 min of reduction a second series of interferograms was taken. Reduction was then continued for an additional 40 min at which time the flow of synthesis gas was restored. The reaction/reduction cycle was repeated a total of seven times. Spectra for six of these cycles are shown in Fig. 5—experimental difficulties precluded obtaining spectra for the fourth cycle. At the end of the seventh cycle, the catalyst was exposed to a flow of CO at 2.5 atm and 473 K

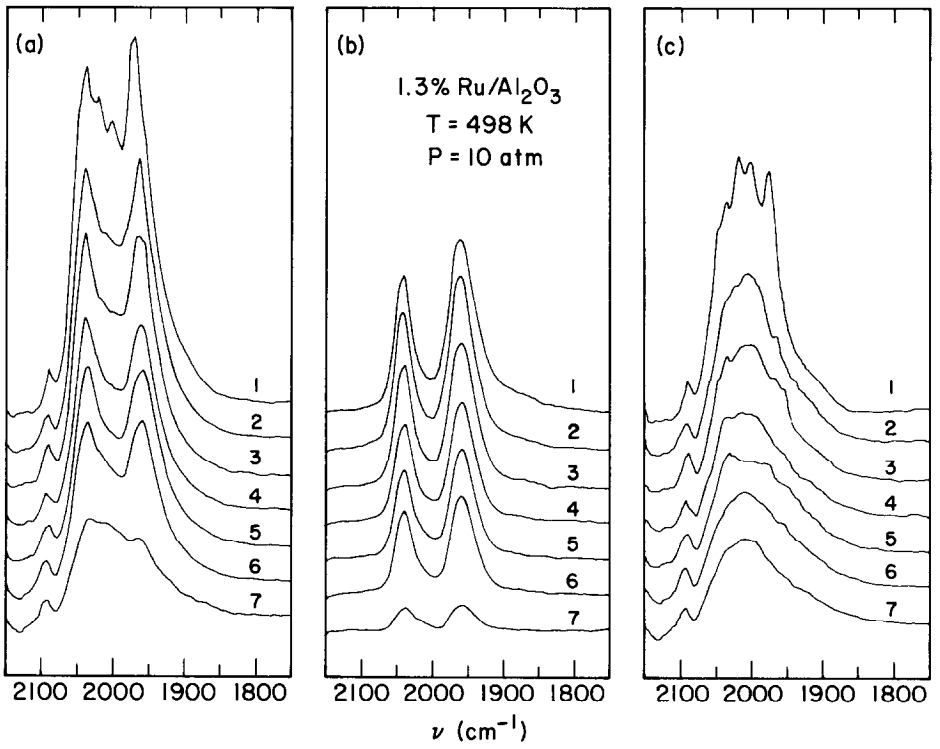

FIG. 5. Infrared spectra obtained during successive reaction—reduction cycles using the 1.3% Ru/Al_2O_3 catalyst: (a) during reaction at 498 K, 10 atm, $H_2/CO = 3$; (b) following reduction in H_2 at 10 atm and 498 K for 10 min; (c) difference between the spectra taken under the conditions give in (a) and (b); spectra 1–3 correspond to cycles 1–3; spectra 4–7 correspond to cycles 5–8; between cycles 7 and 8 the catalyst was exposed to 2.5 atm of CO at 473 K and then reduced in 10 atm of H_2 at 573 K for 12 hr.

for 8 hr and then reduced in flowing H_2 at 10 atm and 573 K for 12 hr. Following this procedure, a regular reaction/reduction cycle was carried out. Spectra taken during this cycle are also shown in Fig. 5. An additional set of spectra were obtained using the 3.0% Ru/Al_2O_3 catalyst. Figure 6a illustrates these results. For the sake of comparison, spectra taken with the 1.3% Ru/Al_2O_3 catalyst during the seventh reaction/reduction cycle are shown in Fig. 6b.

The spectra of the 1.3% Ru/Al_2O_3 catalyst taken under reaction conditions, shown in Fig. 5a, exhibit a broadband at 2010 cm^{-1} and two sharper bands located at 2040 and 1960 cm^{-1}. Based on previous studies (*11–13*), these bands can be assigned to linearly adsorbed CO. The broadband at 2010 cm^{-1} is due to monoadsorbed CO (Ru–CO), and the bands at 2040 and 1960 cm^{-1} are due to diadsorbed CO (OC–Ru–CO). The latter form of CO is associated with either isolated Ru atoms or small clusters, which strongly interact with oxygen in the support (*5, 13*). Reduction of the catalysts causes a complete removal of the monoadsorbed CO leaving behind only the diadsorbed form (Fig. 5b). This structure is stable to H_2 reduction at temperatures below 548 K and hence the intensity of the bands at 2040 and 1960 cm^{-1} are the same under reaction and reduction conditions. As a consequence, it is possible to subtract the spectra in Fig. 5b from those in Fig. 5a to obtain a well-resolved spectrum of the monoadsorbed CO. These difference spectra are shown in Fig. 5c. The spectra in Fig. 6a, obtained with the 3% Ru/Al_2O_3 catalyst, are similar to those for the 1.3% Ru/Al_2O_3 catalyst. The primary difference is that there appears to be very little diadsorbed CO on the surface of the 3% Ru/Al_2O_3 catalyst.

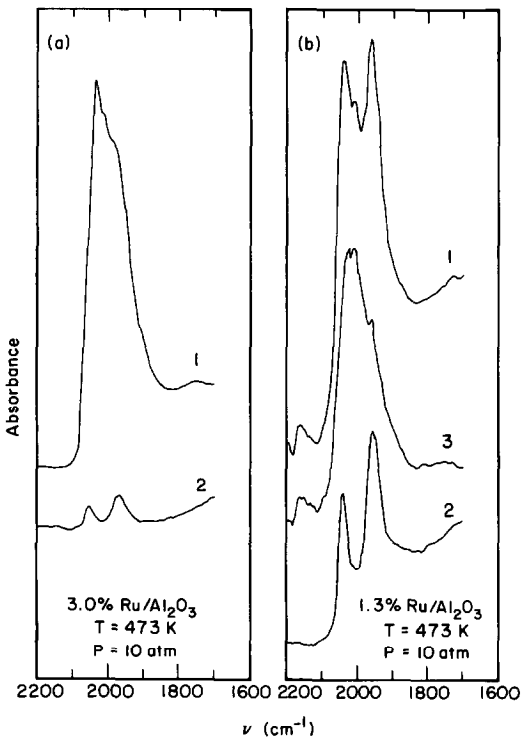

FIG. 6. Infrared spectra obtained under reaction conditions and following reduction: (a) 3.0% Ru/Al_2O_3; (b) 1.3% Ru/Al_2O_3; spectrum 1 was taken during reaction at 473 K, 10 atm, $H_2/CO = 3$; spectrum 2 was taken following reduction in H_2 at 10 atm and 473 K; spectrum 3 is the difference between spectra 1 and 2.

As the 1.3% Ru/Al_2O_3 catalyst is cycled between reaction and reduction conditions, the integrated intensities of the bands shown in Fig. 5 decline (see Table 2) but the positions of the bands do not shift. These observations can be interpreted in the light of a recent *in situ* infrared study of CO hydrogenation over a Ru/Al_2O_3 catalyst, conducted by Kellner and Bell (*13*). These authors observed that the coverage of Ru by linearly adsorbed CO depends only on the CO partial pressure and obeys a Langmuir isotherm for which the adsorption equilibrium constant is given by $K_{CO} = 1.1 \times 10^{-9} \exp(25{,}500/RT)$ atm^{-1}. It was also noted that changes in CO coverage are always accompanied by a downscale shift in the vibrational frequency. The absence of any shift in the frequency of the band for linearly adsorbed CO shown in Fig. 5 indicates that the CO coverage is not altered as the band intensity decreases and implies that the loss in intensity is most likely due to a decrease in Ru dispersion.

The rate of methane formation observed during the infrared studies is also presented

TABLE 2

Effects of Dispersion on the Integrated Band Intensities for Adsorbed CO and the Activity for Methane Synthesis[a]

i	$A_M^{(i)}$ [b]	$A_D^{(i)}$ [b]	$A_M^{(i)}/(A_M^{(i)} + 0.5\,A_D^{(i)})$	r_{C_1} (s^{-1})[c]	$D_{Ru}^{(i)}$ [d]	$N_{C_1}^{(i)}$ (s^{-1})
1	4.20	2.25	0.79	2.25×10^{-4}	0.80[f]	2.81×10^{-4}
2	3.00	2.00	0.75	4.00×10^{-4}	0.60	6.67×10^{-4}
3	2.85	1.60	0.78	5.29×10^{-4}	0.55	9.62×10^{-4}
4	n.a.	n.a.	—	6.14×10^{-4}	—	—
5	2.35	1.45	0.76	6.96×10^{-4}	0.46	15.1×10^{-4}
6	2.18	1.47	0.75	6.96×10^{-4}	0.44	15.8×10^{-4}
7	2.18	1.37	0.77	7.19×10^{-4}	0.43	16.7×10^{-4}
8[g]	1.88	0.70	0.84	7.75×10^{-4}	0.34	22.8×10^{-4}

[a] Catalyst: 1.3% Ru/Al_2O_3; T = 498 K; P 10 atm; H_2/CO = 3.
[b] Arbitrary units.
[c] Based on total number of Ru atoms.
[d] From Eq. (1).
[e] $N_{C_1} = r_{C_1}/D_{Ru}^{(i)}$.
[f] Assumed.
[g] Following exposure to 2.5 atm CO at 473 K for 8 hr and subsequent reduction in H_2 at 10 atm and 573 K for 12 hr.

in Table 2. It is seen that the rate per atom of Ru present in the catalyst increases by nearly a factor of 3.5 as the catalyst is cycled. These data can be used to illustrate the correlation between the specific activity of Ru for methane synthesis and the metal dispersion. To do so, it will be assumed that the surface of Ru is virtually saturated by CO under reaction conditions. This assumption is supported by a calculation of the CO coverage based on the isotherm reported by Kellner and Bell (*13*) and by the fact that the band for linearly adsorbed CO occurs at 2010 cm^{-1}. Next, it is assumed that the integrated absorbances of the bands presented in Figs. 5b and 5c are proportional to the surface coverages by mono- and diadsorbed CO, respectively. This assumption has recently been verified for monoadsorbed CO by Winslow *et al.* (*14*) using a silica-supported Ru catalyst. For the diadsorbed form, this assumption can be inferred from the results presented by Yates *et al.* (*15*) for alumina-supported Rh. Next, it is assumed that the proportionality factors between integrated absorbance and surface concentration are the same for both forms of adsorbed CO. While this assumption has not been substantiated for Ru, it does appear to be valid for Rh (*15*). The catalyst dispersion at the end of each reaction cycle can now be determined from

$$D_{Ru}^{(i)} = D_{Ru}^{(1)} \left[\frac{A_M^{(i)} + 0.5\,A_M^{(i)}}{A_M^{(1)} + 0.5\,A_M^{(1)}} \right], \qquad (1)$$

where $D_{Ru}^{(i)}$ is the Ru dispersion and $A_M^{(i)}$ and $A_D^{(i)}$ are the integrated absorbances for the mono- and diadsorbed forms of CO, respectively. The superscript i represents the cycle number.

The specific activity at the end of each cycle can be determined from the rates given in Table 2 and the values of $D_{Ru}^{(i)}$ given by Eq. (1). The value of $D_{Ru}^{(i)}$ has been assumed to be equal to 0.8. The values of N_{C_1} obtained in this manner are presented in Table 2 and illustrated by the square symbols plotted in Fig. 1. Inspection shows that, here too, the points lie along a straight line, the slope of which is nearly the same as those determined for the other two data sets.

DISCUSSION

The data presented in Figs. 1 and 2 clearly demonstrate that the specific activity of Ru for hydrocarbon synthesis declines with increasing dispersion of the metal. A modest decrease in specific activity is observed for dispersions of less than about 0.75 and a much more rapid decrease is found for higher dispersions. Figure 1 also shows that over the lower dispersion range, the slope of the decrease in specific activity with dispersion found in the present studies is in excellent agreement with that observed by King (*4*). Moreover, it appears that, over the range of temperatures and reactant partial pressures examined, the slope is nearly independent of reaction conditions.

A plausible explanation for the decrease in specific activity with increasing dispersion, observed for $0.3 > D_{Ru} > 0.75$, is that the fraction of the surface sites suitable for carrying out the hydrogenation of CO, decreases with increasing dispersion. Such a trend would be expected if Ru atoms at the faces of crystallites were more active than those at the edges or corners (*16–19*). If one considers, for example, that the crystallites are h.c.p. truncated bipyramids, calculations performed by Van Hardeveld and Hartog (*17, 18*) indicate that the fraction of surface sites not occupying edge or corner positions will decrease by a factor of about 3.5 as the crystallite size decreases from 37 to 12 Å (i.e., D_{Ru} increasing from 0.3 to 0.75). While this decrease is smaller than the 7.5-fold decrease in the specific activity, an association of the loss in specific activity with the availability of a particular type of surface site seems plausible.

An alternative interpretation, and the one originally proposed by King (*4*), is that the decrease in specific activity with increasing dispersion may be due to changes in the electronic properties of the particles. Several reasons can be identified for considering this to be a less satisfactory explanation. To begin with, theoretical studies (*19–23*) of the electronic properties of small metal particles show that deviations from the properties of bulk metal occur, primarily, for crystallites smaller than about 20 Å. This critical size corresponds to a dispersion of about 0.5. If electronic effects are assumed to be central to the change in the specific activity of the catalyst, then it would be expected that these effects should be seen primarily for $D_{Ru} > 0.5$. Figure 1 shows this is not to be the case and, in fact, the specific activity continues to rise smoothly as D_{Ru} decreases to zero. A second argument for excluding an interpretation based on electronic effects can be made on the basis of the infrared studies presented here. The spectra in Fig. 5 show that the vibrational frequency of monoadsorbed CO is independent of dispersion; contrary to what would be anticipated if the electronic properties of the particles change to a significant degree with particle size (*19*).

For dispersions greater than about 0.7, the specific activity and olefin-to-paraffin ratio of the products undergo a very rapid decrease with increasing dispersion and the probability of chain growth, α, decreases slightly. At such high dispersions, the average Ru particle size is less than 12 Å, and as a result a substantial fraction of the particles fall within a size range where particle size and metal–support interactions can influence the electronic properties of the particles (*19–23*). One of the effects that might be expected to occur is a reduction in the density of electronic charge in the *d* orbitals protruding from the metal surface. This could lead to a reduction in the degree of back-donation of charge from these orbitals to the π^* antibonding orbitals of chemisorbed CO and, in turn, reduce the degree to which the C–O bond is weakened (*10, 24*). Since the dissociation of molecularly adsorbed CO is considered to be a critical step in the mechanism of hydrocarbon synthesis over Ru (*10, 25*), and since dissociative chemisorption of CO is facilitated by charge transfer to the π^* orbital of adsorbed CO, a reduction in the back dona-

tion of *d* electrons could be regarded as cause for reducing catalyst activity. The decrease in α and olefin-to-paraffin ratio are probably due to other electronic effects, as yet not clearly defined.

It is apparent from Fig. 2 that over the range of dispersions considered in this investigation, the majority of the products distribute along straight lines on plots of ln (N_{C_n}) versus ($n - 1$). As discussed by a number of authors (*9, 10, 25–28*), such plots suggest that the growth of hydrocarbon chains occurs via the stepwise addition of C_1 units. Deviation of the point for C_2 hydrocarbons from the linear distribution can be ascribed to a partial hydrogenolysis of these products to methane (*9*). The data presented in Fig. 3 show that the deviation for the C_{12+} products is sensitive to the flow rate of synthesis gas and to the duration between the initiation of reaction and product analysis. The decrease in the deviation as either the flow rate or the time of reaction is increased suggests that the deviation is caused by a partial adsorption of C_{12+} hydrocarbons on the support. This interpretation is supported by infrared observations (*11, 13*) which show a progressive accumulation of hydrocarbons on the alumina during reaction. By increasing the flow rate of the feed gas, the concentration of hydrocarbons in the gas phase over the catalyst is reduced, and with it, the equilibrium loading of the support. As a consequence, the time required to achieve the equilibrium loading is reduced.

The results presented in Fig. 3, together with the discussion given above, indicate that over the range of dispersions studied here, there is no indication of a cutoff in chain growth associated with particle size, as has recently been suggested by Nijs and Jacobs (*29, 30*). While it is possible that such a cutoff could exist for particles so small that the normal kinetics of chain growth are distorted by the limited availability of C_1 monomer units, clear evidence for such an effect is not yet available. Moreover, the results of this investigation suggest that such very high-dispersion catalysts would exhibit extremely low specific activities.

In the present study the number of surface Ru sites was determined by H_2 chemisorption assuming a stoichiometry of one H atom per surface Ru atom. The infrared results presented in Figs. 5 and 6 suggest, though, that only those sites which adsorb a single CO molecule per site are active in hydrocarbon synthesis. The sites that adsorb two CO molecules per site appear to be catalytically inactive over the temperature range investigated here. These conclusions are identical to those presented previously (*13*), which were arrived at from detailed infrared studies of CO chemisorption on Ru/Al_2O_3 catalysts. Based on the assumption that the extinction coefficients for monoadsorbed and diadsorbed CO are equal, the data presented in Table 2 suggest that roughly 80% of the surface sites are active and, hence, that the specific activities presented in Figs. 1 and 2 are a factor of 1.25 too low.

The data in Fig. 2 indicate further that as the 1.3% Ru/Al_2O_3 catalyst sinters under reaction conditions, the fraction of monoadsorbed CO remains nearly constant. However, extended exposure of the catalyst to CO at elevated temperatures reduces this fraction significantly. The mechanism of Ru sintering is not revealed by these observations, but the trends in band intensities reported in Table 2 suggest that under reaction conditions the metallic particles grow by the agglomeration of both small clusters and metal crystallites. Both processes must be operative if one is to explain the simultaneous attenuation of the integrated absorbances for monoadsorbed and diadsorbed CO, while maintaining a nearly constant ratio of the two adsorbate forms. It is conceivable that the very rapid growth in average particle size observed during CO hydrogenation is facilitated by the exothermicity of the reaction. The release of heat on a particle surface may give rise to an elevation of the particle temperature

well above the average reaction temperature. This could cause the particle to migrate more readily across the support surface than if the particle temperature remained at the average catalyst temperature. At the same time, one might envision the release of individual Ru atoms from small Ru clusters and migration of these atoms to growing microcrystallites. Small clusters would contribute to such a process more readily than larger crystallites since the metal–metal bond energy decreases significantly with decreasing particle size (*20*). These proposed mechanisms of sintering are admittedly speculative and are not supported by independent evidence. It is anticipated, though, that a better interpretation will be possible following further study of this problem.

CONCLUSIONS

The dispersion of Ru on an alumina support has a pronounced effect on the activity of Ru for CO hydrogenation. For dispersions below about 0.7, there is a moderate decrease in the specific activity for synthesis of methane and C_{2+} hydrocarbons with increasing dispersion, but neither the probability of chain growth nor the olefin-to-paraffin ratio of the products is greatly affected. Dispersions above 0.7 exhibit a very rapid decline in the turnover frequencies for the synthesis of all products. This is accompanied by a slight decrease in the chain growth probability and a very dramatic decrease in the olefin-to-paraffin ratio. At all dispersion levels, the distribution of hydrocarbon products with number of carbon atoms is of a log-normal type. The decrease in specific activity with increasing dispersion, for dispersions below 0.7, is attributed to a decrease in the fraction of sites present on planar surfaces of the Ru microcrystallites. The much faster decrease in specific activity, observed for dispersions greater than 0.7, is believed to be due to changes in the electronic properties of the small crystallites with size or to interactions of the crystallites with the support. *In situ* infrared spectra suggest that only those Ru sites which adsorb one linearly bound CO molecule per site are active for CO hydrogenation, whereas those adsorbing two CO molecules per site are not active under the conditions used in this study.

ACKNOWLEDGMENT

This work was supported by the Director, Office of Energy Research, Office of Basic Energy Sciences, Chemical Sciences Division of the U.S. Department of Energy under Contract W-7405-ENG-48.

REFERENCES

1. Vannice, M. A., *J. Catal.* **40,** 129 (1975).
2. Vannice, M. A., *J. Catal.* **44,** 152 (1976).
3. Dalla Betta, R. A., Piken, G. A., and Shelef, M., *J. Catal.* **35,** 54 (1974).
4. King, D. C., *J. Catal.* **51,** 386 (1978).
5. Kuznetsov, V. L., Bell, A. T., and Yermakov, Yu. I., *J. Catal.* **65,** 374 (1980).
6. Grob, K., and Grob, G., *Chromatographia* **5,** 3 (1972).
7. Hicks, R. F., Kellner, C. S., Savatsky, B. J., Hecker, W. C., and Bell, A. T., *J. Catal.* **71,** 216 (1981).
8. Kellner, C. S., and Bell, A. T., *J. Catal.* **67,** 175 (1981).
9. Kellner, C. S., and Bell, A. T., *J. Catal.* **70,** 418 (1981).
10. Bell, A. T., *Catal. Rev. Sci. Eng.* **23,** 203 (1981).
11. Dalla Betta, R. A., and Shelef, M., *J. Catal.* **48,** 111 (1977).
12. King, D. L., *J. Catal.* **61,** 77 (1980).
13. Kellner, C. S., and Bell, A. T., *J. Catal.*, **71,** 296 (1981).
14. Winslow, P., Cant, N., and Bell, A. T., unpublished results.
15. Yates, J. T., Jr., Duncan, T. M., Worley, S. D., and Vaughn, R. W., *J. Chem. Phys.* **70,** 1219 (1979).
16. Poltorak, O. M., and Boronin, V. S., *Russ. J. Phys. Chem.* **40,** 1436 (1966).
17. Van Hardeveld, R., and Hartog, F., *Surf. Sci.* **15,** 189 (1969).
18. Van Hardeveld, R., and Hartog, F., *Advan. Catal.* **22,** 75 (1972).
19. Basset, J. M., and Ugo, R., *in* "Aspects of Homogeneous Catalysis" (R. Ugo, Ed.), Vol. 3. Reidel, Boston, 1977.
20. Burton, J. J., *Catal. Rev. Sci. Eng.* **9,** 209 (1974).
21. Baetzold, R. C., *Advan. Catal.* **25,** 1 (1976).
22. Muetterties, E. L., Rhodin, T. N., Bond, E., Brucher, C. F., and Pretzer, W. R., *Chem. Rev.* **79,** 91 (1979).

23. Anderson, J. R., "Structure of Metallic Catalysts." Academic Press New York, 1975.
24. Broden, G., Rhodin, T. N., and Brucher, C., *Surf. Sci.* **59,** 593 (1976).
25. Biloen, P., and Sachtler, W. M. H., *Advan. Catal.* **30,** 165 (1981).
26. Friedel, R. A., and Anderson, R. B., *J. Amer. Chem. Soc.* **72,** 1212, 2307 (1950).
27. Henrici-Olivé, G. and Olivé, *Angew. Chem. Int. Ed. Engl.* **15,** 136 (1976).
28. Madon, R. J., *J. Catal.* **57,** 183 (1979).
29. Nijs, H. H., and Jacobs, P. A., *J. Catal.* **65,** 328 (1980).
30. Nijs, H. H., and Jacobs, P. A., *J. Catal.* **66,** 401 (1980).